The Flavor of Cosmology

Benjamin Lillard,^{1,*} Michael Ratz,^{1,†} Tim M.P. Tait,^{1,2,‡} and Sebastian Trojanowski^{1,3,§}

¹Department of Physics and Astronomy, University of California, Irvine, CA 92697-4575 USA ²Institute of Physics and Astronomy, University of Amsterdam, The Netherlands ³National Centre for Nuclear Research, Hoża 69, 00-681 Warsaw, Poland

Abstract

We discuss the cosmology of models in which the standard model Yukawa couplings depend on scalar field(s), often referred to as flavons. We find that thermal corrections of the flavon potential tend to decrease the Yukawa couplings, providing an important input to model-building. Working in the specific framework of Froggatt–Nielsen models, we compute the abundance of flavons in the early universe generated both via freeze-in and from coherent oscillations induced by thermal corrections to their potential, and discuss constraints on flavon models from cosmology. We find that cosmology places important constraints on theories containing flavons even for regions of parameter space inaccessible to collider searches.

^{*} blillard@uci.edu

[†] mratz@uci.edu

[‡] ttait@uci.edu

[§] strojano@uci.edu & Sebastian.Trojanowski@ncbj.gov.pl

I. INTRODUCTION

Despite its tremendous phenomenological success, the Standard Model of particle physics (SM) leaves open a number of key questions. In particular, the surprisingly large hierarchies manifest in the masses of the fermions and their peculiar pattern of mixing seems to hint at an underlying dynamical structure. Many extensions of the SM have been proposed to address this so-called flavor puzzle [1–10]. Among them, arguably one of the most compelling proposals is the idea by Froggatt and Nielsen [2] that the pattern of masses and mixings reflects the charges of a spontaneously broken, family-non-universal U(1)_{FN} symmetry.

While Froggatt-Nielsen (FN) models can arise from a variety of different ultraviolet (UV) theories, they share two common ingredients: an Abelian U(1)_{FN} symmetry and the presence of at least one flavon S – a scalar field whose vacuum expectation value (VEV) spontaneously breaks U(1)_{FN}. The couplings of S to pairs of SM fermions are dictated by the U(1)_{FN} charges of the latter, and the mass hierarchies and mixing patterns are encoded in terms of powers of the ratio ε between $\langle S \rangle$ and the UV completion scale Λ , but are relatively insensitive to the scale of Λ itself. Typically, $\varepsilon \equiv \langle S \rangle / \Lambda$ is of the order of the Cabbibo angle, and the entries of the Yukawa couplings are (up to order one coefficients descending from the UV theory) given by powers of ε .

In this study, we examine the cosmological constraints on models containing flavons. Our focus is the parameter region in which Λ is large, as suggested by constraints from flavor observables, but the flavon excitations are comparatively light. In this regime, late decays of the flavon pose two possible threats to standard cosmology: they may spoil the successful predictions from primordial nucleosynthesis (BBN) and/or dilute the primordial baryon asymmetry to an unacceptable level. We show that cosmology leads to interesting bounds on the parameter space.

In fact, though our explicit calculations are performed in the specific framework of Froggatt–Nielsen models, the constraints we derive apply to a much broader range of frameworks in which the Yukawa interactions are determined by VEV's. In particular, our discussion reveals that the so-called moduli problem [11, 12] typically discussed in the context of string model building is more severe than previously appreciated.

This paper is organized as follows. In Section II we review some of the basic properties of FN models relevant for our analysis. In Section III we discuss various flavon production mechanisms in the early Universe, and in Section IV, derive cosmological bounds. We conclude in Section V. Some of the technical details are presented in more detail in a number of appendices.

II. FROGGATT-NIELSEN

The low-energy effective Lagrange density of an FN model contains a global $U(1)_{FN}$ symmetry such that the Yukawa couplings for the SM quarks are realized as non-renormalizable interactions containing the appropriate power of S to maintain $U(1)_{FN}$,

$$\mathscr{L}_{\text{FN}} = \sum_{i,j=1}^{3} y_{ij}^{u} \left(\frac{S}{\Lambda}\right)^{n_{ij}^{u}} \overline{Q}_{i} \widetilde{\Phi} u_{j} + \sum_{i,j=1}^{3} y_{ij}^{d} \left(\frac{S}{\Lambda}\right)^{n_{ij}^{d}} \overline{Q}_{i} \Phi d_{j} + \text{h.c.}, \qquad (1)$$

where, $y_{ij}^{u/d}$ are dimensionless couplings presumably of order unity, and Φ , Q_i , u_i and d_j

denote the SM Higgs and quark fields. The integer powers $n_{ij}^{u/d}$ derive from the U(1)_{FN} charges of the respective quarks. In a convention in which S carries U(1)_{FN} charge $Q_{\rm FN}(S) = -1$, one has $n_{ij}^u = -Q_{\rm FN}(Q_i) + Q_{\rm FN}(u_j)$ and $n_{ij}^d = -Q_{\rm FN}(Q_i) + Q_{\rm FN}(d_j)$, respectively. The U(1)_{FN} symmetry forbids direct couplings between Higgs and most of the SM quarks and leptons. A non-zero VEV for S results in hierarchical Yukawa couplings given by $\varepsilon = v_S/(\sqrt{2}\Lambda)$ raised to the appropriate power which, together with appropriate order one coefficients $y_{ij}^{u/d}$ reproduce the observed fermion masses and mixings [13–18]. Reproducing the quark masses and mixings fix, to some extent, ε and the U(1)_{FN} charges, but leave the UV scale Λ and the flavon mass m_{σ} as free parameters.

In this work, we choose to focus exclusively on the quarks, as they typically dominate flavon phenomenology and leave exploration of analogous constructions for the leptons to future work. Because of the freedom in the $y_{ij}^{u/d}$ coefficients, the FN charges are not uniquely determined by the observed quark masses and mixings. This leaves some model-dependence in the flavon couplings. In Appendix A, we present two representative choices of parameters based on $\varepsilon = 0.23$ and reproducing the observed quark masses and mixings, which we use in our numerical studies.

There are a variety of UV complete models whose low energy limit is Equation (1) (see e.g. [19–21]). While the precise details of the UV completion are typically not very important for our purposes, they can serve as a guide for interesting regions of parameter space. In most explicit models, the U(1)_{FN} charges of the (left-chiral) spinors describing SM fermions all have the same sign, and the U(1)_{FN} symmetry is anomalous (however, see [22]). It is well known that pseudo-anomalous U(1)_{FN} symmetries can arise from string theory [14, 18], with the anomalies cancelled by the Green–Schwarz mechanism [23], and the VEV of the flavon set by a (field-dependent) Fayet–Iliopoulos term [24, 25]. In such cases, Λ is expected to be of the order of the Planck scale M_P . On the other hand, in string models the fields determining the couplings, often referred to as moduli, usually have masses well below Λ . While explicit string models tend to have richer structure than the FN model, analogous constraints also typically apply to them.

There are also models in which the flavor scale is as low as $\Lambda \sim \text{TeV}$ such that flavons can in principle be produced at the Large Hadron Collider (LHC) [26, 27]. For lighter masses, there are typically strong bounds from flavor changing neutral current (FCNC) processes (for recent discussion see e.g. [28]) with typical limits of order $\sqrt{\Lambda m_{\sigma}} \gtrsim \text{few TeV}$ [29]. We will consider masses as low as $m_{\sigma} \gtrsim 10 \,\text{GeV}$, and Λ in the range $\text{TeV} \lesssim \Lambda \lesssim M_{\text{P}}$.

A. $U(1)_{FN}$ -Breaking

In order to generate the Yukawa interactions, one spontaneously breaks the $U(1)_{FN}$ symmetry by engineering a potential for the flavon,

$$\mathcal{Y}_S = -\mu_S^2 |S|^2 + \lambda_S |S|^4 + \lambda_{S\Phi} |S|^2 |\Phi|^2 + U(1)_{FN} \text{ breaking terms},$$
 (2)

such that the flavon acquires a non-zero VEV v_S ,

$$S = \frac{1}{\sqrt{2}}(v_S + \sigma + i\rho). \tag{3}$$

The mixed quartic $\lambda_{S\Phi}$ between the flavon and the Higgs is unavoidable, but we will assume it is small enough that it can be safely ignored in our analysis. If present, it induces mixing

between the flavon and the Higgs boson after both $U(1)_{FN}$ and electroweak symmetry-breaking, and contributes to the mass parameters for both flavon and Higgs.

Soft U(1)_{FN} breaking terms are included to give mass to the pseudoscalar flavon ρ , lifting it from the effective theory. A very light ρ would be ruled out, whereas $m_{\rho} \sim m_{\sigma}$ would result in an order one change in the cosmological bounds we derive below. We focus on the limit $m_{\rho} \gg m_{\sigma}$ to simplify our analysis. Of course, invoking explicit U(1)_{FN} breaking raises the possibility of a loss of predictivity such that the explanation of the fermion mass hierarchy and mixing structure will be spoiled. In Appendix B, we construct a model in which U(1)_{FN} is replaced by a discrete \mathbb{Z}_N symmetry, which allows for the ρ to be heavier than σ while maintaining the FN mechanism.

B. Flavon Couplings

Before the electroweak phase transition (EWPT), the flavon couples to pairs of quarks and the Higgs boson via non-renormalizable interactions obtained from Equation (1) by expanding S around its VEV,

$$\mathcal{L}_{\text{EWPT}}^{\text{before}} \supset \sum_{i,j} \frac{g_{ij}^u}{\Lambda} \sigma \, \overline{Q}_i \widetilde{\Phi} u_j + \sum_{i,j} \frac{g_{ij}^d}{\Lambda} \sigma \overline{Q}_i \widetilde{\Phi} d_j , \qquad (4)$$

where

$$g_{ij}^u \simeq \frac{y_{ij}^u}{\sqrt{2}} n_{ij}^u \varepsilon^{n_{ij}^u - 1} \quad \text{and} \quad g_{ij}^d \simeq \frac{y_{ij}^d}{\sqrt{2}} n_{ij}^d \varepsilon^{n_{ij}^d - 1} .$$
 (5)

After EWPT, the Higgs can be replaced by its VEV, $v_{\rm EW} \simeq 246\,{\rm GeV}$, producing renormalizable interactions. In the quark mass basis $u_{\rm L,R}$ and $d_{\rm L,R}$, the flavon couplings are given by

$$\mathcal{L}_{\text{EWPT}} \supset \tilde{g}_{ij}^u \, \sigma \, \bar{u}_{\text{L},i} \, u_{\text{R},j} + \tilde{g}_{ij}^d \, \sigma \, \bar{d}_{\text{L},i} \, d_{\text{R},j} \,, \tag{6}$$

where

$$\tilde{g}_{ij}^{u} \simeq \frac{1}{2\varepsilon} \frac{v_{\text{EW}}}{\Lambda} \left[U_{u}^{\dagger}(n^{u}Y_{u})W_{u} \right]_{ij} \quad \text{and} \quad \tilde{g}_{ij}^{d} \simeq \frac{1}{2\varepsilon} \frac{v_{\text{EW}}}{\Lambda} \left[U_{d}^{\dagger}(n^{d}Y_{d})W_{d} \right]_{ij} .$$
 (7)

The $Y_{u/d} \equiv y_{ij}^{u/d} \varepsilon^{n_{ij}^{u/d}}$ are the Yukawa interactions, which are diagonalized as usual by unitary matrices $U_{u/d}$ and $W_{u/d}$ via the biunitary transformation $Y_{u/d}^{\text{diag}} = U_{u/d}^{\dagger} Y_{u/d} W_{u/d}$. The object $(nY) \equiv n_{ij} Y_{ij}$ is not generally diagonal in the mass basis, leading the flavon to mediate tree level flavor-changing neutral currents.

Note that all interactions between the flavon and quarks are suppressed by at least one power of Λ , and vanish in the limit of very large flavor scale.

III. FLAVON PRODUCTION IN THE EARLY UNIVERSE

Flavons can be produced in the early universe through a variety of processes. As usual, the key question is whether or not the flavon chemically equilibrates with the SM plasma in the early Universe. If the Hubble expansion rate H exceeds the rate of flavon production at all relevant times, $\Gamma_{\text{SM}\leftrightarrow\sigma} < H$, the flavon is too weakly coupled to achieve thermal equilibrium in the early universe, and the flavon abundance will be determined by out-of-equilibrium processes.

At high temperatures (above the EWPT), the flavon's interactions with quarks are non-renormalizable, and fall out of equilibrium at a temperature $T_{\rm dec}$, defined by $H(T_{\rm dec}) = n_X \langle \sigma v \rangle$, where the thermally averaged cross section in the limit $T \gg m_\sigma$ is $\langle \sigma v \rangle \sim (g_{ij}^{u/d})^2/\Lambda^2$, and where $n_X \simeq n_X^{\rm eq} = \zeta(3)T^3/(4\pi^3)$ for relativistic bosons. It is convenient to write $H = T^2/M_H$ with $M_H = M_P/(1.66\sqrt{g_*^\rho}) \approx 1.4 \times 10^{17}$ GeV for the radiation-dominated universe. Up to $\mathcal{O}(1)$ factors,

$$T_{\rm dec} \approx \frac{10^2 \Lambda^2}{M_H \sum_{ij} \left| g_{ij}^{u/d} \right|^2} \sim 10^{15} \,\,{\rm GeV} \left(\frac{\Lambda}{10^{15} \,\,{\rm GeV}} \right)^2 \,.$$
 (8)

Typically the highest relevant temperature correspond to the reheating temperature after inflation, T_R . For $T_R < T_{\text{dec}}$, the flavon abundance is set by out-of-equilibrium processes:

- For most of the parameter space, the dominant production mechanism is from model-independent thermal corrections to the flavon potential.
- Flavons are also produced through the scattering of standard model particles, in parallel production of gravitinos [30–32] and axinos [33] in supersymmetric scenarios, and more generally with "freeze-in" production [34]. One interesting subtlety arises because the flavon couplings become effectively renormalizable after the EWPT, leading to two distinct epochs of freeze-in production.
- There are potentially additional model-dependent production mechanisms. For example, there may be direct couplings between the flavon and inflaton, leading to flavon production when the inflaton decays. Or the flavon could experience a brief period of equilibrium during the reheating period, in which the temperature can attain much larger values than T_R , though this is typically balanced by efficient dilution in the fast expanding Universe. We neglect these contributions to the yield, leading to results which are conservative in the sense that their inclusion could only lead to more stringent cosmological constraints.

We examine the model-independent processes in more detail in the following subsections.

A. Finite Temperature Corrections to the Scalar Potential

At temperatures $T \gtrsim \mathcal{O}(m_{\sigma})$, thermal corrections to the effective flavon potential $\mathscr{V}(\sigma)$ supplement the freeze-in contribution to the flavon yield by inducing oscillations in σ . The thermal corrections to the potential of the flavon are analogous to those to the dilaton

potential [35, 36]. This discussion applies to the case in which the flavon is not in thermal equilibrium. For a discussion of equilibrated flavons, see e.g. [37]. The crucial point is that the free energy receives contributions from the Yukawa couplings y, which we derive in Appendix C,

$$\mathcal{F} = \gamma y^2 T^4 + \alpha T^4 \frac{\sigma}{\Lambda} + \dots , \qquad (9)$$

where $\gamma = 5/96$. As the latter depend on the flavon, this leads to a thermal potential of the flavon of the form

$$\mathscr{V}_{\text{eff}}(\sigma, T) = \gamma T_Y T^4 + \alpha T^4 \frac{\sigma}{\Lambda} + \frac{m_{\sigma}^2(T)}{2} \sigma^2 + \frac{\kappa}{3!} \sigma^3 + \frac{\lambda_S}{4} \sigma^4 + \dots , \qquad (10)$$

where, $\kappa \sim m_{\sigma}^2/v_s$, $T_Y = \operatorname{tr}\left(Y_u^{\dagger}Y_u + Y_d^{\dagger}Y_d\right)$ and

$$\alpha = \gamma \frac{\partial T_Y}{\partial \varepsilon} \sim 10^{-2} \,. \tag{11}$$

The α term in Equation (10) drives the flavon away from its zero-temperature minimum towards smaller values.

Qualitatively, the flavon gets driven away from its T = 0 minimum until it gets stopped by the mass term or Hubble friction,

$$\Delta \sigma \simeq -\alpha \frac{T^4}{\Lambda m_{\text{eff}}^2} \quad \text{where } m_{\text{eff}}^2 = 6H^2 + m_{\sigma}^2 \,.$$
 (12)

As the temperature decreases, the flavon undergoes oscillations around the T=0 minimum, which behave like nonrelativistic matter.

More quantitatively, the energy density in the form of flavon oscillations follows the equation of motion, $\ddot{\sigma} + (3H + \Gamma_{\sigma})\dot{\sigma} + \partial \mathcal{V}_{\text{eff}}/\partial \sigma = 0$, which together with $\dot{T} \approx -HT$ becomes

$$H^2 T^2 \frac{\mathrm{d}^2 \sigma}{\mathrm{d}T^2} - \Gamma_\sigma H T \frac{\mathrm{d}\sigma}{\mathrm{d}T} + \alpha \frac{T^4}{\Lambda} + m_\sigma^2 \sigma + \frac{1}{2} \kappa \sigma^2 + \lambda_s \sigma^3 \approx 0.$$
 (13)

Under the assumptions that $T \gg \Gamma_{\sigma}$ and $\lambda_S \ll 1$, this equation of motion can be approximated by

$$H^2 T^2 \frac{\mathrm{d}^2 \sigma}{\mathrm{d}T^2} + \alpha \frac{T^4}{\Lambda} + m_\sigma^2 \sigma \approx 0.$$
 (14)

The exact solution to Equation (14) is detailed in Appendix D, but it is instructive to discuss limiting cases. At high temperatures $H \gg m_{\sigma}$, the two asymptotic solutions for $\sigma(T)$ scale as $\sigma \propto T$ and $\sigma \propto \ln T$, while at low-to-intermediate temperatures $\Gamma_{\sigma} \ll H \lesssim m_{\sigma}$ the solutions in a radiation-dominated universe $(H = T^2/M_H)$ approach the form (see Figure 5(b) in Appendix D)

$$\sigma(T) = \sigma_0 \left(\frac{T}{T_*}\right)^{3/2} \cos\left(\frac{1}{2}\frac{T_*^2}{T^2} - \varphi\right) \quad \text{with } T_* \equiv \sqrt{m_\sigma M_H} , \qquad (15)$$

where φ denotes a phase that is determined by the initial conditions.

The amplitude σ_0 is highly sensitive to the boundary conditions if $T_R \gtrsim T_*$, but tends to $\sigma_0 \propto T_R^{5/2}$ if $T_R \ll T_*$. This scaling with T_R continues at high temperature if one assumes that the flavon σ begins at rest at the minimum of its *finite* temperature potential $\mathscr{V}(T=T_R)$ rather than at $\mathscr{V}(T=0)$. A different boundary condition $\sigma(T_R) = \dot{\sigma}(T_R) = 0$ gives an amplitude proportional to $\ln(T_R/T_*)$ at high temperatures. We adopt a rather conservative *lower* bound on the flavon yield based on the $\sigma(T_R) = \dot{\sigma}(T_R) = 0$ boundary condition. A more general discussion of the initial conditions is provided in Appendix D.

From the amplitude of the oscillations in (15), the yield from flavon oscillations reads

$$Y^{\text{osc}} \approx \alpha^2 \frac{A_* M_{\text{P}} m_{\sigma}}{\Lambda^2} \left[\frac{M_H(T_R)}{m_{\sigma}} \right]^{3/2} \times \begin{cases} \left(\frac{T_R}{T_*} \right)^5 & \text{if } T_R \lesssim T_* ,\\ 2.1 \ln^2 \left(\frac{T_R}{T_*} \right) & \text{if } T_R \gg T_* . \end{cases}$$

$$(16)$$

Note that it is possible for the energy density in the flavon oscillations to exceed that of the relativistic thermal bath, causing an early matter-dominated epoch in the evolution of the universe. In this event the assumption $H = T^2/M_H$ ceases to apply, and the evolution of $\sigma(T)$ is no longer described by Equation (15). However, in the absence of an additional entropy production from other sources, the flavon yield at the time of decay is still described by Equation (16).

B. High Temperature Freeze-In Production

At temperatures above the electroweak phase transition, flavon production occurs via $2 \to 2$ scattering through the nonrenormalizable operators, Eqs. (4) and (5). For every pair of quarks Q_i and u_j , there are six processes by which the flavon σ are produced,

$$\overline{Q}_i + u_j \to \sigma + H , \qquad \overline{Q}_i + H^{\dagger} \to \sigma + \overline{u}_j , \qquad H^{\dagger} + u_j \to \sigma + Q_i ,
Q_i + \overline{u}_j \to \sigma + H^{\dagger} , \qquad Q_i + H \to \sigma + u_j , \qquad H + \overline{u}_j \to \sigma + \overline{Q}_i . \tag{17}$$

A similar set of processes exists for the down-type quarks. Adding them together and solving the respective Boltzmann equation one obtains the ultraviolet (UV) contribution to the total yield of flavon $Y_{\sigma} = n_{\sigma}/s$, where n_{σ} is the flavon number density, and s is the entropy density. For a given process involving up or down quarks from the ith and jth generation, it reads

$$Y_{ij}^{u/d, \text{UV}} = \frac{3 \left| g_{ij}^{u/d} \right|^2 A_* M_P m_\sigma}{64\pi^5} \int_{x_{\text{min}}}^{x_{\text{max}}} dx \left(16 - 3x^2 \right) K_2(x) + 8x K_1(x) + 3x^2 K_0(x) , \quad (18)$$

where $A_* \equiv 45/(2\pi^2 g_*^S 1.66 \sqrt{g_*^{\rho}})$. The limits of integration are given by $x_{\min} = m_{\sigma}/T_R$ and $x_{\max} = m_{\sigma}/T_{\text{EWPT}}$, where T_{EWPT} is the temperature of the EWPT, taken to be $T_{\text{EWPT}} = 100$ GeV. Precise modeling of the dynamics of EWPT is beyond the scope of this work.

At small values of x_{\min} the integrand in Equation (18) is approximated by a power series, $\mathcal{I}(x) \approx (32/x^2) - 6 + \mathcal{O}(x^2)$, while for $m_{\sigma} \gtrsim 2 T_{\text{EWPT}}$, the integral is insensitive to the precise value of x_{\max} . As a consequence it is reasonable to approximate

$$Y_{ij}^{u/d,\,\text{UV}} \approx \frac{3|g_{ij}^{u/d}|^2 A_* M_P T_R}{2\pi^5}$$
 (19)

in the range $T_{\text{EWPT}} \ll m_{\sigma} \ll T_{R}$.

C. Freeze-In Below the Electroweak Phase Transition

For a low reheating temperature, $T_R \lesssim \mathcal{O}(\text{TeV})$, a significant contribution to the flavon yield comes from freeze-in after the EWPT via the renormalizable interactions, Equation (6). In particular, as long as $m_{\sigma} \geq (m_i + m_j)$, where m_i are the quark masses, $2 \to 1$ scattering is the leading order flavon production mechanism. For much smaller flavon masses $m_{\sigma} < (m_i + m_j)$ the $q\bar{q} \to \sigma$ scattering is kinematically forbidden, and flavon production is driven instead by $2 \to 2$ scattering such as $q\bar{q} \to \sigma g$. Here, we assume that the flavon is heavy enough that the $2 \to 1$ scattering is sufficient to describe low-temperature flavon yield.

The infrared (IR) contribution to the flavon yield from a given $2 \to 1$ scattering is

$$Y_{ij}^{(u/d), \text{IR}} \approx \frac{3A_* M_P}{16\pi^3 m_\sigma} \left| \tilde{g}_{ij}^{u/d} \right|^2 \left(1 - 2 \frac{m_i m_j}{m_\sigma^2} \right) \times \sqrt{1 - \frac{(m_i + m_j)^2}{m_\sigma^2}} \sqrt{1 - \frac{(m_i - m_j)^2}{m_\sigma^2}} \int_{x_{\text{min}}}^{\infty} dx \, x^3 \, K_1(x) , \qquad (20)$$

where $x_{\min} = m_{\sigma}/T_{\text{EWPT}}$ and we effectively replace $x_{\max} \to \infty$ which is a good approximation provided $m_{\sigma} \gtrsim \mathcal{O}(\text{GeV})$. For low flavon masses, $m_{\sigma} \lesssim T_{\text{EWPT}}$, one can set $x_{\min} \to 0$ and the remaining integral is equal to $3\pi/2$. The IR contribution to the yield is obtained after summing over all the relevant processes $Y_{\sigma}^{\text{IR}} = \sum_{ij} Y_{ij}^{u,\text{IR}} + \sum_{ij} Y_{ij}^{d,\text{IR}}$. The contribution from the subprocess with top quarks in the initial state is negligible since their number density is highly Boltzmann suppressed after the EWPT.

We also neglect the dynamical effects associated with the EWPT by approximating a constant value for the Higgs VEV and using the zero temperature flavon couplings for all $T < T_{\rm EWPT} = 100$ GeV.

D. Flavon Yield in the Early Universe

The total flavon yield is the sum of the contribution from flavon oscillations together with the IR and UV freeze-in production:

$$Y_{\sigma} = \sum_{ij} \left(Y_{ij}^{u,\text{UV}} + Y_{ij}^{u,\text{IR}} + Y_{ij}^{d,\text{UV}} + Y_{ij}^{d,\text{IR}} \right) + Y^{\text{osc}} . \tag{21}$$

In Figure 1, we show the flavon yield Y_{σ} as a function of T_R and m_{σ} , with flavon couplings that correspond to the parameter set (FN charges 1) in Appendix A for $\Lambda = 10^{15}$ GeV. All three contributions to the yield scale uniformly as Λ^{-2} .

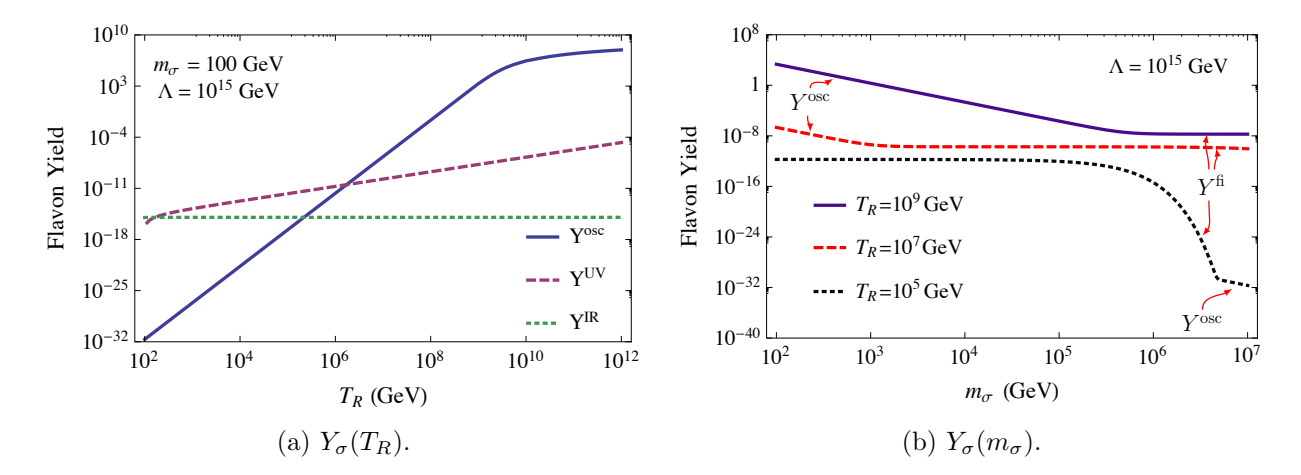


FIG. 1. The total flavon yield as (a) a function of T_R for a fixed value of $m_{\sigma}=100\,\mathrm{GeV}$ and (b) as a function of m_{σ} for fixed values of $T_R=10^5, 10^7, 10^9\,\mathrm{GeV}$. In both plots we take $\Lambda=10^{15}\,\mathrm{GeV}$: all contributions to the flavon yield scale as Λ^{-2} . In the right panel, we indicate whether the yield is driven primarily by Y^{osc} or by the freeze-in contribution $Y^{\mathrm{fi}}=Y^{\mathrm{UV}}+Y^{\mathrm{IR}}$. For $T_R=10^5\,\mathrm{GeV}$, the exponential suppression of Y^{fi} can be seen for $m_{\sigma}>T_R$, while Y^{osc} obeys a simple power law in this regime.

For large reheating temperatures, the freeze-in yield is subdominant to the oscillatory contribution Y^{osc} , particularly for light flavons. The situation is reversed at lower temperatures $T_R \ll \sqrt{m_\sigma M_H}$, as can be seen in Figure 1(a). Here Y^{UV} becomes the largest contribution, provided T_R and m_σ are still large compared to the electroweak scale. This behavior is easily explained from Equations (16) and (18): the freeze-in yield scales as $Y^{\text{UV}} \propto T_R$, while the oscillatory component scales much more dramatically as $Y^{\text{osc}} \propto T_R^5$.

For light flavons with $m_{\sigma} \lesssim 100$ GeV, $Y^{\rm IR}$ surpasses $Y^{\rm UV}$ for small reheating temperatures $T_R \lesssim \mathcal{O}(\text{TeV})$, but is otherwise negligible compared to $Y^{\rm UV}$ and $Y^{\rm osc}$. This can be understood from Equations (18) to (20) in the limit of $T_R \gg T_{\rm EWPT}$ and large flavon mass,

$$Y_{ij}^{(u/d), \text{IR}} \lesssim \frac{v_h^2}{m_\sigma T_R} Y_{ij}^{(u/d), \text{UV}} \ll Y_{ij}^{(u/d), \text{UV}}.$$
 (22)

We close with a discussion of some of the effects not captured in our calculations:

- Our estimates treat the distribution functions according to Maxwell-Boltzmann statistics, which is questionable in the relativistic $T \gg m_{\sigma}$ limit. To assess the error introduced by this simplification, we examine the impact of correcting the statistical factors for one subprocess in Appendix E, and find that it impacts the outcome by an $\mathcal{O}(1)$ factor.
- The leading-order freeze-in yield is expected to be further modified when the effects from thermal quark masses $m_q^2(T) \sim \frac{1}{6}g_s^2T^2$ are included (for a review, see for example [38]). At high temperatures the effect is modest, but for light flavons at low temperatures $T_R \lesssim T_{\rm EWPT}$ the thermal effects can restrict the phase space for the $2 \to 1$ scattering $q\bar{q} \to \sigma$ that determines $Y^{\rm IR}$. We therefore restricted ourselves to scenarios with $T_R \gtrsim 1$ TeV.

• There are corrections to the low-temperature freeze-in contribution from next-to-leading order QCD processes such as $q\bar{q} \to \sigma g$. These are enhanced by a color factor and are kinematically allowed even when $m_{\sigma} < 2m_q(T)$. Even in the case of a light flavon with $m_{\sigma} \lesssim 100$ GeV and reheating temperature $T_R \sim 1$ TeV, the QCD corrections are expected to be not larger than an $\mathcal{O}(1)$ factor.

These simplifications and formally higher order corrections can be large, leading to an $\mathcal{O}(1)$ uncertainty in our results for the yield. While beyond the scope of our work, it would be interesting to pursue refined estimates for the flavon yield in the future.

IV. COSMOLOGICAL CONSTRAINTS ON LATE-TIME DECAYS OF FLAVONS

The flavons produced in the early universe will eventually decay back to SM degrees of freedom. Depending on the epoch in which this occurs, it can have dramatic consequences for cosmology. For $m_{\sigma} \gtrsim 10\,\mathrm{GeV}$, the primary concern is the possibility of spoiling the successful predictions from big bang nucleosynthesis (for a similar analysis on light flavons see [29]). Late-time energy injection from flavon decays could also cause spectral distortions in the Cosmic Microwave Background (CMB) radiation [39, 40], although these constraints are typically less severe than the ones from BBN provided the decaying particle is heavy enough. In addition, even if flavon decays happen earlier, they might cause a significant entropy production that dilutes a primordial baryon asymmetry to values inconsistent with observations. In the following, we discuss constraints on the flavon that can be deduced from these processes.

A. Flavon Decays

The flavon lifetime depends on whether or not the electroweak symmetry is broken. In particular, before the EWPT when the flavon interactions are described by Equations (4) to (5), the decay width into 3-body final state, $\sigma \to \Phi \overline{Q}_i u_i$, is given by

$$\Gamma_{ij}^{u/d,\,\text{UV}} = \frac{N_c \,|g_{ij}^{u/d}|^2}{3 \, 64 \, \pi^3} \frac{m_\sigma^3}{\Lambda^2} \,. \tag{23}$$

On the other hand, if this decay rate is smaller than the Hubble rate at the time of the EWPT, $\Gamma_{ij}^{u/d,\,\mathrm{UV}} < H(t_{\mathrm{EWPT}})$, the flavon lifetime is effectively determined by the renormalizable couplings Equations (6) to (7). The 2-body flavon decay width into pairs of quarks, $\sigma \to u_i \bar{u}_j + u_j \bar{u}_i$, then reads [27]

$$\Gamma_{ij}^{u,\text{IR}} = \frac{3 m_{\sigma}}{16 \pi} \frac{v_{\text{EW}}^2}{\Lambda^2} \left[\frac{\left[m_{\sigma}^2 - (m_i + m_j)^2 \right] \left[m_{\sigma}^2 - (m_i - m_j)^2 \right]}{m_{\sigma}^4} \right]^{1/2} \\
\times \left\{ \left(|\widetilde{g}_{ij}^u|^2 + |\widetilde{g}_{ji}^u|^2 \right) \left(1 - \frac{m_i^2 + m_j^2}{m_{\sigma}^2} \right) - 4 \operatorname{Re}(\widetilde{g}_{ij}^u \widetilde{g}_{ji}^u) \frac{m_i m_j}{m_{\sigma}^2} \right\} ,$$
(24)

and similarly for down-type quarks. In particular, as can be seen in Equations (A3a) to (A5a), flavon decays into a pair of top quarks are possible when kinematically allowed.

Note that a flavon coupling to a pair of top quarks is typically induced through the non-trivial basis change from u_3 and Q_3 to the mass eigenstates $t_{L/R}$ (see Equation (A3) and Equation (A5)).

The total flavon decay width Γ_{σ} is the sum of the various flavor combinations in the channels discussed above. It determines the flavon decay temperature, T_{σ} from $\Gamma_{\sigma} \simeq H(T_{\sigma})$,

$$T_{\sigma} = \left(\frac{90}{\pi^2 g_{*,\rho}}\right)^{1/4} \sqrt{M_{\rm P} \Gamma_{\sigma}} \stackrel{\rm IR}{\sim} 0.2 \cdot \frac{v_{\rm EW}}{\Lambda} \sqrt{M_{\rm P} m_{\sigma}}. \tag{25}$$

An additional suppression of T_{σ} on top of the simple scaling in Equation (25) is obtained for $m_{\sigma} < m_t$ since then the dominant decay channels of flavon involving the top quark are forbidden. For cases in which the flavon temporarily dominates the energy density of the universe, T_{σ} is the temperature at which the radiation dominated epoch is restored when the flavon decays.

B. Big Bang Nucleosynthesis Constraints

If the lifetime of the flavon, τ_{σ} , exceeds $\sim 0.1-1$ sec, its decays are subject to potentially stringent constraints from its potential to destroy the successful predictions of the BBN (for recent reviews see Refs [41, 42]), e.g. by producing electromagnetic and/or hadronic showers which destroy light nuclei (see, e.g., [43–47] and references therein). As a result, there are bounds from BBN on the yield of sufficiently long-lived flavons:

- For large enough Y_{σ} and $\tau_{\sigma} \lesssim 10^2 \, \mathrm{sec}$, hadronic particles produced in σ decays can cause $p \leftrightarrow n$ interconversion, affecting the ⁴He mass fraction, Y_p , by changing the neutron-to-proton ratio. At later times, for $\tau_{\sigma} \gtrsim 10^2 \, \mathrm{sec}$, injected high-energy hadrons are no longer effectively stopped in thermal plasma [46] and hadrodissociation processes take place. As a result, the BBN constraints become much stronger in this regime and typically come from deuterium overproduction caused by hadrodissociation of ⁴He.
- Electromagnetic cascades initiated by decays of flavons typically get equilibrated by scatterings of injected high-energy γ -rays on background photons that lead to e^+e^- pair production. However, for lower temperatures, pair production becomes inefficient and photodissociation of D or even ⁴He can occur for $\tau \gtrsim 10^4$ sec and $\tau \gtrsim 10^6$ sec, respectively leading to constraints comparable to those from hadronic decays.

Constraints on late-decaying particles from BBN have recently been revisited [48] to include up-to-date observational data concerning the primordial abundances of light elements and improved determinations of the rates of relevant nuclear reactions. Particularly relevant are new stringent limits on the D/H ratio based on significantly reduced observational uncertainties [49] and updates to Y_p incorporating the recent study of emission lines in both infrared and visible wavelengths in 45 extragalactic HII regions¹ [50].

¹ This measurement was initially claimed to be inconsistent with standard BBN predictions [50], but more recent analysis indicates no statistically meaningful discrepancy [51].

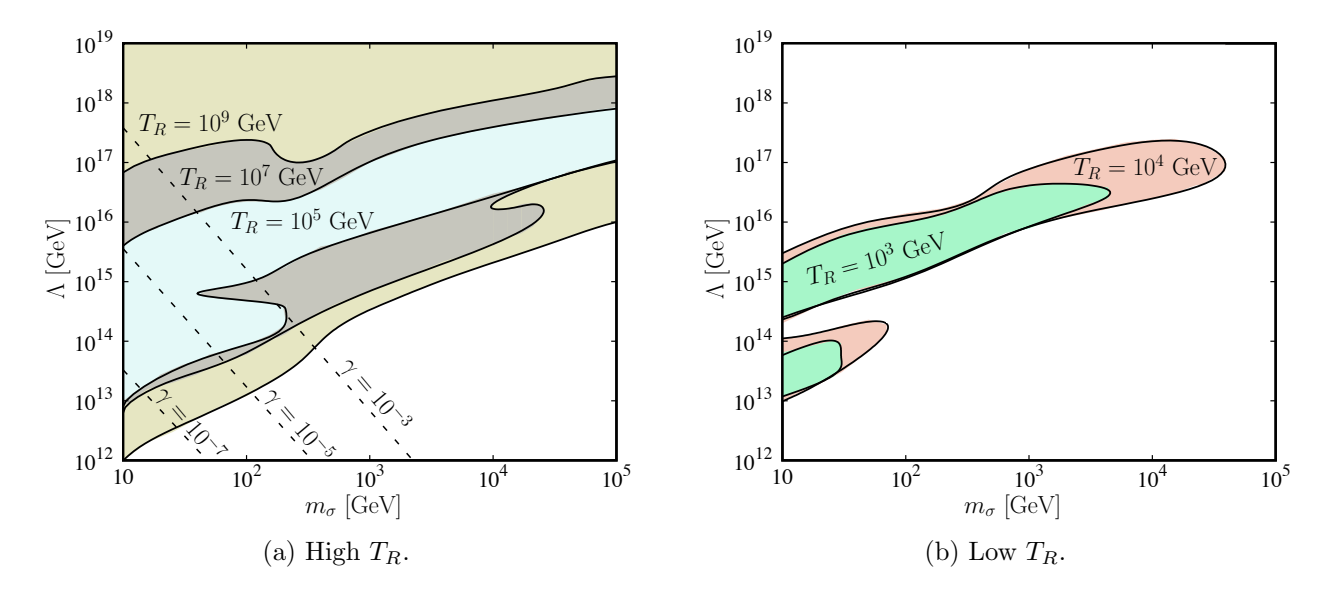


FIG. 2. Big Bang Nucleosynthesis constraints on late-time flavon decays in the (m_{σ}, Λ) plane. In (a) the light blue (gray, olive) shaded areas correspond to regions in the parameter space excluded for $T_R = 10^5 \,\text{GeV}$ ($10^7 \,\text{GeV}$, $10^9 \,\text{GeV}$). In (b) the limits are shown for $T_R = 10^3 \,\text{GeV}$ and $10^4 \,\text{GeV}$ as green and red shaded areas, respectively.

In the left panel of Figure 2 we show the BBN constraints on the (m_{σ}, Λ) plane for several values of the reheating temperature from $T_R = 10^5$ to 10^9 GeV. For a given m_{σ} , the BBN limits exclude a window of Λ starting where the flavon lifetime corresponds to the onset of BBN, $\tau_{\sigma} \gtrsim 0.1-1$ sec and ending when Λ becomes large enough that the flavon yield decreases to the point that its decays become irrelevant for BBN. For $T_R = 10^9$ GeV, this upper boundary occurs for $\Lambda > M_{\rm P}$. The detailed shape of the exclusion regions for $m_{\sigma} \leq 100$ GeV correspond to the interplay of multiple observables, with the lower Λ (i.e., lower τ_{σ}) constraints dominated by $p \leftrightarrow n$ interconversion and the larger values excluded by hadrodissociation processes. For $T_R = 10^3$ GeV to 10^4 GeV the situation is qualitatively the same, as can be seen in the right panel of Figure 2(a). A new feature for these lower reheat temperatures is an intermediate range of $\Lambda \sim 10^{14}$ GeV for which the flavon yield is already low enough to avoid the limits from $p \leftrightarrow n$ interconversion processes, while its lifetime is short enough that the constraints from hadrodissociation do not apply, resulting in a channel of allowed parameter space.

If the reheating temperature exceeds the freeze-out temperature, Equation (8), the flavon could enter thermal equilibrium at some stage of the cosmological evolution and might dominate the energy density of the universe at later times when it becomes nonrelativistic. In this case, we require $T_{\sigma} > T_{\rm BBN}$ in order to prevent the early stages of BBN from proceeding during a matter dominated epoch.

The exclusion bounds shown in Figure 2 depend on the choice of FN charges $n_{ij}^{u/d}$ and the associated order one coefficients $y_{ij}^{u/d}$. For natural models realizing the FN mechanism, the variations in the flavon couplings are of order one (see Appendix A). Thus, the model-dependence of the bounds is typically at most of the same order as the theoretical uncertainties discussed in Section III. We verify that the two example choices of FN charges (FN charges 1) and (FN charges 2) result in exclusion bounds which differ by a fac-

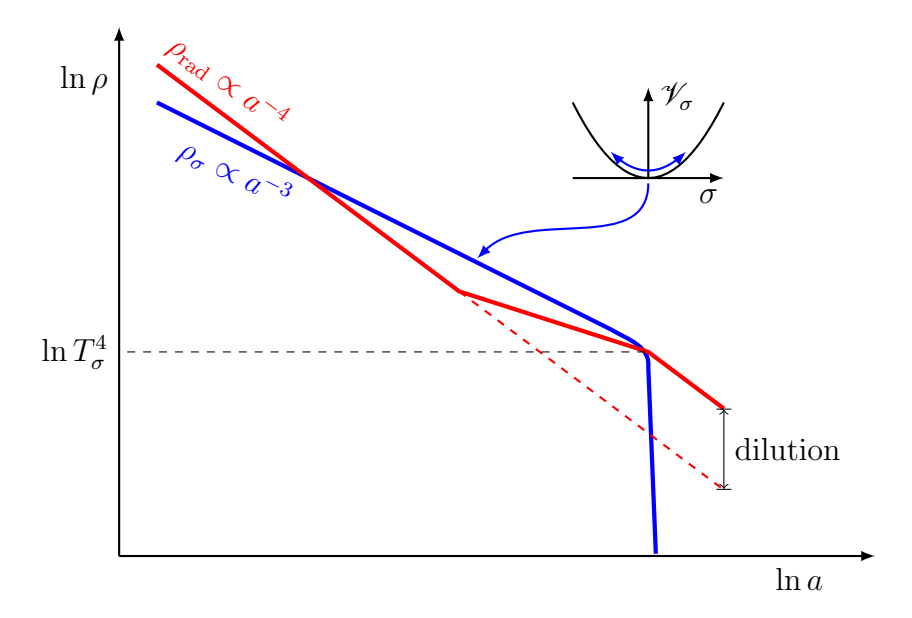


FIG. 3. Cartoon of the moduli problems associated with weakly coupled flavons.

tor of order unity, and choose to simplify the presentation by focusing on the assignment (FN charges 1).

As noted in [48], if one adopts the initial determination of the ⁴He mass fraction from [50], the resulting discrepancy with respect to the standard BBN predictions can be explained by an additional hadronic energy injection from decays of a new heavy particle with a lifetime of $\tau \lesssim 10^2$ sec (in order to avoid exclusion bounds from hadrodissociation processes), whose yield is close to the upper limit from $p \leftrightarrow n$ interconversions. Interestingly, this scenario can be realized by late-time decays of the weakly coupled flavon. For $m_{\sigma} = 1$ TeV (used for illustration purposes in [48]), the discrepancy disappears provided $\Lambda \sim 10^{15}$ GeV and $T_R \sim (10^6 - 10^7)$ GeV.

C. Dilution of the Baryon Asymmetry of the Universe

In cases where the flavon dominates the energy density of the universe, its subsequent decays can produce significant entropy and effectively wash out baryons, leading to a reduced value of the primordial baryon asymmetry, as illustrated schematically in Figure 3. In this regime, the flavon yield is typically dominated by the contribution from field oscillations described in Equation (16). We assume that the flavon does not reach equilibrium, $T_{\text{dec}} > T_R$. The respective dilution factor (see Figure 3 for an illustration), $\gamma \leq 1$, is given by the ratio between the radiation entropy density at T_{σ} calculated as if there were no flavon, s_{before} , and the radiation entropy density after the flavon decay, s_{after} (see, e.g., [37])

$$\gamma \equiv \frac{s_{\text{before}}}{s_{\text{after}}} \simeq \min \left[\frac{3}{4} T_{\sigma} \frac{s^{\text{ini}}}{\rho_{\sigma}^{\text{ini}}}, 1 \right] = \min \left[\frac{3 T_{\sigma}}{4 m_{\sigma} Y_{\sigma}^{\text{ini}}}, 1 \right] , \qquad (26)$$

where $\rho_{\sigma}^{\rm ini}$, $s^{\rm ini}$ and $Y_{\sigma}^{\rm ini}$ are the flavon energy density, entropy density and flavon yield evaluated at a time when the initial amplitude of σ field oscillations was set (see Appendix D

for details). Typical values of γ are shown in Figure 2(a) in the (m_{σ}, Λ) plane for $T_R = 10^9$ GeV.

The precise impact of flavon decays on the baryon asymmetry depends on the specific model of baryogenesis, in particular on the temperature at which the baryon asymmetry is generated. Scenarios such as thermal leptogenesis [52], for which the baryon asymmetry is at best linear in T_R , are difficult to reconcile with weakly coupled flavons, since $Y_{\sigma}^{\text{osc}} \propto T_R^5$ (cf. Equation (16)). In particular, for the maximal CP violation, the baryon-to-entropy ratio in the thermal leptogenesis scenario is given by [53]

$$\frac{n_b}{s} \lesssim \gamma \times 6 \times 10^{-11} \times \left(\frac{m_{N_1}}{10^{11} \text{ GeV}}\right) , \qquad (27)$$

where m_{N_1} is the mass of the right-handed neutrino. As can be seen in Figure 2(a), a light flavon with $\Lambda \sim 10^{12}$ GeV (at which scale it does not equilibrate for $T_R = 10^9$ GeV) is characterized by very small values of γ . In this case, the observed value of $n_b/s \simeq 9 \times 10^{-11}$ [54] can only be reproduced for unreasonably large values of m_{N_1} . This constraint is complementary to the bounds from BBN discussed in Section IV B.

D. Implications for Model Building

While our results are derived in the specific framework of FN models, our discussion of thermal corrections to the flavon potential applies to a more general class of models where the quark Yukawa couplings are field-dependent. Such scenarios include string and supergravity models, in which the Yukawa couplings are moduli-dependent, and σ can stand for any of the moduli, as well as bottom-up models in which flavor is encoded through dynamics.

As derived in Appendix C, the free energy becomes smaller for decreasing Yukawa couplings, and thermal corrections tend to drive the effective Yukawa couplings smaller at high temperatures. This is analogous to the statement that thermal corrections tend to switch off the gauge couplings [35, 36].

What are the implications of these effects? As far as string model building is concerned, we find that the so-called moduli problem [11, 12] is often worse than appreciated. It has been argued (see e.g. [55] and references therein) that the oscillations of moduli are suppressed if the moduli become trapped at symmetry-enhanced points. However, we find that if the gauge and/or Yukawa couplings depend on these moduli, they get pushed away from their T=0 minimum by an amount given in Equation (12), even if trapped there during inflation. We stress that these amplitudes are model-independent.

Let us close with a comment on other scenarios with varying Yukawa couplings. It has been argued (see e.g. [56]) that in the SM (extended by an FN sector) there might be a first order phase transition if at temperatures of the order $T_{\rm EW}$ the flavon has an expectation value of the order Λ . However, we find that thermal corrections drive the flavon to smaller values. It would thus be interesting to assess the viability of such scenarios with the thermal corrections taken into account.

V. CONCLUSIONS

We have studied the phenomenology of models in which the SM Yukawa couplings are set by the VEV(s) of some field(s), σ . Such fields are referred to as flavons or moduli in

the literature. When these flavons are weakly coupled, they evade detection by collider experiments, but can nevertheless produce large effects in cosmology. Along the way, we have uncovered an important disagreement with previous analyses stating that the flavon coupling to a pair of top quarks vanishes. Rather, we find that it is often rather sizable as detailed in Appendix A.

In the early universe, flavons are produced either in scatterings of the SM particles, or result from coherent oscillations triggered by thermal deformations of their potential. While the first production mode is very similar to the one of gravitinos, axinos and other ultraweakly coupled particles, to our knowledge the second production mode has not been discussed in the literature and we find that it dominates in large portions of the parameter space of interest.

Our analysis provides some key lessons. First, even if the couplings of the flavon are suppressed by a mass scale Λ that is large enough to render collider experiments irrelevant, cosmology nonetheless places restrictions on the mass of the flavon. If m_{σ} is rather small, late decays of the flavon may spoil BBN. Even if the flavon decays before BBN, it may (depending on the specific model of baryogenesis) unacceptably dilute the baryon asymmetry of the universe. Both of these issues have been previously discussed in the context of the so-called moduli problem. However, our results cast doubt on some of the proposed solutions to this problem when the Yukawa couplings of the SM fermions depend on the modulus' in question. In more detail, it is not sufficient to provide a mechanism that fixes the moduli at the minimum of the zero-temperature potential during inflation, since they will still typically get pushed away after reheating and thus jeopardize cosmology.

It is also worth mentioning that the finite temperature corrections to the potential are such that flavons get driven to values at which the Yukawa couplings are *smaller*. It will thus be interesting how scenarios in which the Yukawa couplings are taken to be larger in the early universe get modified after our model-independent corrections have been taken into account.

Beyond the specifics of theories in which a modulus controls the SM notion of flavor, our results illustrate the importance of cosmology as a window into particle physics at energy scales far beyond the reach of current collider or conventional astrophysical probes.

ACKNOWLEDGMENTS

We are grateful to Mu-Chun Chen, Tilman Plehn, and Arvind Rajaraman for insightful discussions, and Marco Drewes for correspondence. This work is supported in part by NSF Grant No. PHY-1620638 and PHY-1719438. S.T. is supported in part by the Polish Ministry of Science and Higher Education under research grant 1309/MOB/IV/2015/0 and by the National Science Council (NCN) research grant No. 2015-18-A-ST2-00748.

Appendix A: Realistic Flavon Couplings

We consider two representative choices of the FN charges that are commonly used in the literature [18, 56]:

$$Q_{\text{FN}}^{(1)}(\overline{Q}_i) = (3, 2, 0) , \ Q_{\text{FN}}^{(1)}(u_i) = (5, 2, 0) , \ Q_{\text{FN}}^{(1)}(d_i) = (4, 3, 3) ,$$
 (FN charges 1)

$$Q_{\text{FN}}^{(2)}(\overline{Q}_i) = (3, 2, 0) , \ Q_{\text{FN}}^{(2)}(u_i) = (4, 1, 0) , \ Q_{\text{FN}}^{(2)}(d_i) = (3, 2, 2) .$$
 (FN charges 2)

Both sets differ by U(1)_{FN} charges assigned to SU(2)_L singlet fields with the first choice corresponding to systematically larger values, but are consistent with observations for an appropriate choice of the $\mathcal{O}(1)$ coefficients $y_{ij}^{u/d}$ in Equation (1).

In both scenarios the FN charges of the up-type third generation quarks vanish, $Q_{\text{FN}}(Q_3) =$ $Q_{\rm FN}(u_3)=0$, as dictated by the top Yukawa coupling, $(Y_u)_{33}\sim 1$. This, in turns, implies that before EWPT there are no tree-level flavon interactions with a pair of top quarks. On the other hand, as we shall see in more detail below, after EWPT a nonzero $\sigma t\bar{t}$ coupling gets induced upon rotation to the mass basis. Although this effect can be non-negligible, the dominant flavon couplings are typically the off-diagonal $\sigma t\bar{c}$ and the diagonal σbb . In particular, in the flavor basis they correspond to $\sigma \overline{Q}_3 u_2$ and $\sigma \overline{Q}_3 d_3$ couplings, respectively, *i.e.*, they are proportional to ε (ε ²) and ε ² (ε ³) for the first (second) set of the FN charges.

While these two charge assignments lead to flavon couplings with parametrically different dependence on ε , this difference is partially compensated by the $y_{ij}^{u/d}$ necessary to reproduce observations. We determine these coefficients by performing a fit to the values [57] of the quarks masses, the CKM matrix entries and the Jarlskog invariant with the use of the Multinest scanning tool [58]. The Yukawa couplings are evolved under the renormalization group using the SPheno [59, 60] implementation of the SM via the SARAH package [61]. Below we present the results for $y_{ij}^{u/d}$ at high-energy scale 10^{10} GeV. With those coefficients determined, the flavon couplings above EWPT can then be obtained from Equation (5). The couplings at and below the scale of EWPT, $\tilde{g}^{u/d}$, are obtained upon rotation to the mass basis as shown in Equation (7).

Since our aim is to explore realistic model points and examine how these two commonly used charge assignments differ in terms of their cosmological bounds, we keep only the leading digits in the fit points and leave careful exploration of the allowed ranges of parameters for future work. In our numerical studies, it turns out that the differences in the cosmological constraints from both sets of charges and flavon couplings are never larger than a factor of a few, and thus have minor impact on the exclusion plots. Thus, in Sections III and IV we present results based on (FN charges 1).

Our fit determines:

• For the choice (FN charges 1), the $\mathcal{O}(1)$ coefficients at the scale $10^{10}\,\mathrm{GeV}$ are

$$y^{u} \simeq \begin{pmatrix} 0.3 + 0.3i & -0.2 + 0.5i & 0.2 - 0.2i \\ -0.3 + 0.2i & -0.4 + 0.5i & 0.5 - 0.3i \\ 0.4 - 0.3i & -0.4 - 0.9i & 0.3 + 0.5i \end{pmatrix},$$

$$y^{d} \simeq \begin{pmatrix} 0.4 + 0.2i & 0.2 - 0.2i & 0.2 - 0.3i \\ 0.1 - 0.6i & 1.0 - 0.1i & -0.2 - 0.4i \\ -0.4 + 0.3i & -0.4 + 0.6i & 0.4 + 0.5i \end{pmatrix}.$$
(A2a)

$$y^{d} \simeq \begin{pmatrix} 0.4 + 0.2 \, \mathrm{i} & 0.2 - 0.2 \, \mathrm{i} & 0.2 - 0.3 \, \mathrm{i} \\ 0.1 - 0.6 \, \mathrm{i} & 1.0 - 0.1 \, \mathrm{i} & -0.2 - 0.4 \, \mathrm{i} \\ -0.4 + 0.3 \, \mathrm{i} & -0.4 + 0.6 \, \mathrm{i} & 0.4 + 0.5 \, \mathrm{i} \end{pmatrix} . \tag{A2b}$$

The flavon couplings at the scale of EWSB in the quark mass basis are

$$\widetilde{g}^{u} \simeq \frac{v_{\text{EW}}}{2\Lambda} \begin{pmatrix} (-4-0.2\,\mathrm{i}) \times 10^{-4} & (0.9-\mathrm{i}) \times 10^{-3} & (7-2\,\mathrm{i}) \times 10^{-2} \\ (-0.6-5\,\mathrm{i}) \times 10^{-4} & (0.1-50\,\mathrm{i}) \times 10^{-3} & 0.3+0.5\,\mathrm{i} \\ (2-3\,\mathrm{i}) \times 10^{-3} & 0.7-0.4\,\mathrm{i} & 0.09-0.05\,\mathrm{i} \end{pmatrix}, (A3a)$$

$$\widetilde{g}^{d} \simeq \frac{v_{\text{EW}}}{2\Lambda} \begin{pmatrix} (-2-4\,\mathrm{i}) \times 10^{-4} & (0.5-3\,\mathrm{i}) \times 10^{-4} & (-2+2\,\mathrm{i}) \times 10^{-3} \\ (-1-6\,\mathrm{i}) \times 10^{-4} & (-10+2\,\mathrm{i}) \times 10^{-3} & (-7-7\,\mathrm{i}) \times 10^{-3} \\ (7-7\,\mathrm{i}) \times 10^{-3} & (-2-2\,\mathrm{i}) \times 10^{-3} & -0.2+0.2\,\mathrm{i} \end{pmatrix}. (A3b)$$

$$\widetilde{g}^{d} \simeq \frac{v_{\text{EW}}}{2\Lambda} \begin{pmatrix} (-2-4\,\mathrm{i}) \times 10^{-4} & (0.5-3\,\mathrm{i}) \times 10^{-4} & (-2+2\,\mathrm{i}) \times 10^{-3} \\ (-1-6\,\mathrm{i}) \times 10^{-4} & (-10+2\,\mathrm{i}) \times 10^{-3} & (-7-7\,\mathrm{i}) \times 10^{-3} \\ (7-7\,\mathrm{i}) \times 10^{-3} & (-2-2\,\mathrm{i}) \times 10^{-3} & -0.2+0.2\,\mathrm{i} \end{pmatrix} . \quad (A3b)$$

• For the choice (FN charges 2), the $\mathcal{O}(1)$ coefficients at the scale 10^{10} GeV are

$$y^{u} \simeq \begin{pmatrix} 0.4 + 0.4 i & 0.1 + 0.1 i & 0.2 - 0.2 i \\ -0.1 + 0.3 i & 0.1 + 0.2 i & 0.4 - 0.5 i \\ 0.8 - 0.1 i & -0.3 - 0.5 i & 0.2 + 0.5 i \end{pmatrix},$$
(A4a)

$$y^{d} \simeq \begin{pmatrix} 0.5 + 0.1 \, \mathrm{i} & 0.2 - 0.1 \, \mathrm{i} & 0.2 - 0.1 \, \mathrm{i} \\ 0.6 - 0.1 \, \mathrm{i} & 0.5 - 0.1 \, \mathrm{i} & -0.1 - 0.2 \, \mathrm{i} \\ -0.1 + 0.1 \, \mathrm{i} & -0.1 + 0.1 \, \mathrm{i} & 0.1 + 0.1 \, \mathrm{i} \end{pmatrix} . \tag{A4b}$$

The flavon couplings at the scale of EWSB in the quark mass basis read

$$\widetilde{g}^{u} \simeq \frac{v_{\text{EW}}}{2\,\Lambda} \begin{pmatrix} (-1+9\,\mathrm{i}) \times 10^{-4} & (4+5\,\mathrm{i}) \times 10^{-3} & (-40+2\,\mathrm{i}) \times 10^{-2} \\ (-40-4\,\mathrm{i}) \times 10^{-4} & 0.02+0.2\,\mathrm{i} & -0.5+0.2\,\mathrm{i} \\ (50-6\,\mathrm{i}) \times 10^{-3} & -0.5-\mathrm{i} & -0.3+0.2\,\mathrm{i} \end{pmatrix} , \quad (A5a)$$

$$\widetilde{g}^{u} \simeq \frac{v_{\text{EW}}}{2\Lambda} \begin{pmatrix} (-1+9\,\mathrm{i}) \times 10^{-4} & (4+5\,\mathrm{i}) \times 10^{-3} & (-40+2\,\mathrm{i}) \times 10^{-2} \\ (-40-4\,\mathrm{i}) \times 10^{-4} & 0.02+0.2\,\mathrm{i} & -0.5+0.2\,\mathrm{i} \\ (50-6\,\mathrm{i}) \times 10^{-3} & -0.5-\mathrm{i} & -0.3+0.2\,\mathrm{i} \end{pmatrix}, \quad (A5a)$$

$$\widetilde{g}^{d} \simeq \frac{v_{\text{EW}}}{2\Lambda} \begin{pmatrix} (-30-3\,\mathrm{i}) \times 10^{-4} & (10-7\,\mathrm{i}) \times 10^{-4} & (5-6\,\mathrm{i}) \times 10^{-3} \\ (5+7\,\mathrm{i}) \times 10^{-4} & 0.01-0.02\,\mathrm{i} & -0.02+0.2\,\mathrm{i} \\ (20-8\,\mathrm{i}) \times 10^{-3} & (-3-4\,\mathrm{i}) \times 10^{-3} & 0.2+0.2\,\mathrm{i} \end{pmatrix}. \quad (A5b)$$

We note that in contrast to statements in the literature, the 3–3 entries in the couplings of \widetilde{q}^u , i.e. the couplings of the flavon to the t quark does not vanish. Rather, using the values of [27] we obtain a coupling of magnitude 0.1 (see Equation (A3a)) while for the choice (FN charges 2) we obtain couplings larger than 0.3 (see Equation (A5a)). These results are not optimized, and it may be possible to arrive at larger or smaller couplings to the top quark for different sets of the $\mathcal{O}(1)$ coefficients.

Appendix B: Lifting the ρ Mass

In this appendix, we present a model which lifts the pseudoscalar ρ from the spectrum without additional distortion to the phenomenology. If the global symmetry $U(1)_{FN}$ were to be exact, ρ would be a Goldstone boson, and thus massless. On the other hand, if one were to explicitly break the $U(1)_{FN}$ symmetry such that ρ acquires a mass, this would generically allow for operators which contribute to the SM Yukawa interactions and destroy the FN mechanism.

One option could be to gauge $U(1)_{FN}$, so that ρ is eaten as the longitudinal mode of the associated gauge boson, but in that case the massive gauge boson itself complicates the discussion. For an unsuppressed gauge coupling, the gauge boson would be heavy, but would

mediate additional interactions between the flavon and the SM matter fields. For a very small gauge coupling, these interactions would be suppressed, but the gauge boson would be light, and could play an important role in low energy phenomenon.

A better option is to replace $U(1)_{FN}$ by a discrete \mathbb{Z}_N symmetry, where N is even and larger than twice the largest Froggatt-Nielsen charge. The charge assignment for the \mathbb{Z}_N coincides with the one of $U(1)_{FN}$. In this case, the flavon potential (2) is given by

$$\mathcal{V}_{S} = -\mu_{S}^{2} S^{*} S + \frac{\lambda}{4} (S^{*} S)^{2} + \frac{\kappa}{\Lambda^{N-4}} \left(S^{N} + (S^{*})^{N} \right) + \frac{\eta}{\Lambda^{N-2}} (S^{*} S)^{1+N/2} , \qquad (B1)$$

where we omit other higher order couplings and κ and η are dimensionless parameters. The presence of the κ term shifts the VEV of the flavon, and more importantly leads to a mass term for the would-be-Goldstone mode $\rho = \text{Im } S/\sqrt{2}$,

$$m_{\rho}^2 \sim \frac{v_S^N}{\Lambda^{N-2}}$$
, where $v_S \sim \sqrt{\frac{\mu_S^2}{\lambda}}$. (B2)

As discussed in the main text, we consider small λ . At the same time, we want the flavon to settle around 0.23Λ , so $\mu_S^2 \ll \Lambda^2$. In this regime the U(1)_{FN} breaking terms can be more important than the U(1)_{FN} conserving terms. For example, for the parameters

$$\Lambda = 10^{10} \, {\rm GeV} \,, \quad N = 16 \,, \quad \lambda = 10^{-9} \,, \quad \kappa = 0.008 \quad {\rm and} \quad \eta = 0.4 \,,$$

we obtain a minimum at $\operatorname{Re} S = 0.23 \cdot \Lambda$ with

$$m_{\sigma}^2 \simeq 1.67 \cdot 10^{11} \, {\rm GeV}^2$$
 and $m_{\rho}^2 \simeq 2.37 \cdot 10^{11} \, {\rm GeV}^2$,

provided that $\mu_S^2 = 1.78 \cdot 10^{10} \,\text{GeV}^2$, which realizes the desired pattern of masses.

Appendix C: Free Energy of a Relativistic Gas of Fermions and Bosons with Yukawa Interactions

In this appendix, we compute the thermal correction to the free energy due to Yukawa couplings. To this end, we consider a massless Dirac fermion Ψ , a massless complex scalar ϕ , and the interaction Lagrangian

$$\mathcal{L}_{\text{Yukawa}} = -y \overline{\Psi} P_{\text{L}} \Psi \phi + \text{h.c.}$$
 (C1)

The free energy of a relativistic gas of fermions and bosons with Yukawa interactions can be computed using basic methods of thermal field theory. Following the discussion of [38]

around Equation (5.116), we obtain the leading-order correction to the free energy as

$$\Delta \mathcal{F} = -|y|^2 \sum_{\{p\}} \int_{\{q\}} \int_{k} \delta^{(4)}(p - q - k) \operatorname{Tr} \left[\frac{1}{p} P_{L} \frac{1}{q} P_{R} \frac{1}{k^2} \right].$$
(C2)

By convention [38], the momenta of the fermions are indicated by curly brackets. The integrand of the 2-loop integral (C2) can be rewritten as

$$P = \operatorname{Tr}\left[\frac{1}{p}P_{L}\frac{1}{q}P_{R}\frac{1}{(p-q)^{2}}\right] = \frac{\operatorname{Tr}\left[P_{L}\not p \not q\right]}{p^{2}q^{2}(p-q)^{2}}$$

$$= \frac{2p \cdot q}{p^{2}q^{2}(p-q)^{2}} = \frac{p^{2}+q^{2}-(p-q)^{2}}{p^{2}q^{2}(p-q)^{2}} = \frac{1}{q^{2}k^{2}} + \frac{1}{p^{2}k^{2}} - \frac{1}{p^{2}q^{2}},$$
(C3)

where k = p - q is the 4-momentum of the scalar. So we are left with integrals of the type

$$I \equiv \iint_{\{p\}} \underbrace{\int_{k} \frac{1}{p^{2} k^{2}}}_{k} + \underbrace{\int_{\{q\}} \int_{k} \frac{1}{q^{2} k^{2}}}_{\{q\}} - \underbrace{\int_{\{p\}} \int_{\{q\}} \frac{1}{p^{2} q^{2}}}_{\{q\}}$$

$$= 2 \left(\underbrace{\int_{\{p\}} \frac{1}{p^{2}}}_{\{p\}} \right) \cdot \left(\underbrace{\int_{k} \frac{1}{k^{2}}}_{k} \right) - \left(\underbrace{\int_{\{p\}} \frac{1}{p^{2}}}_{\{p\}} \right) \cdot \left(\underbrace{\int_{\{q\}} \frac{1}{q^{2}}}_{\{q\}} \right) . \tag{C4}$$

To evaluate them, we use the standard integrals in [38],

$$I_T(0) = \sum_{p} \frac{1}{p^2} = \frac{T^2}{12} \text{ and } \widetilde{I}_T(0) = \sum_{\{p\}} \frac{1}{p^2} = -\frac{T^2}{24}$$
 (C5)

for bosons and fermions, respectively. This yields the contribution of one set of chiral fermions with Yukawa coupling y to the free energy as

$$\Delta \mathcal{F} = \frac{5|y|^2}{576} T^4 . \tag{C6}$$

Hence, in the SM the contribution of a quark q with Yukawa coupling y_q is given by²

$$\Delta \mathcal{F}_{\text{SM}} \simeq \frac{5 |y_q|^2}{96} T^4 \,. \tag{C7}$$

 $^{^2}$ There is a color factor of 3 and another factor 2 because the Higgs and one of the fermions are $SU(2)_L$ doublets.

Appendix D: Analytic Solution for Flavon Oscillation

In the regime where the flavon decay can be neglected $(H \gg \Gamma_{\sigma})$ and where the universe is radiation-dominated $(H = T^2/M_H)$, the equation of motion (14) can be solved exactly to find the oscillation of the flavon about its zero-temperature minimum. In this appendix we describe the asymptotic solutions for $\sigma(T)$ at high and low temperatures, and show how the amplitude of the flavon oscillations can be derived for a given set of initial conditions.

We define the dimensionless variables ω and z which replace σ and T, such that all of the coefficients in the equation of motion are +1,

$$\omega \equiv \frac{\Lambda}{\alpha M_H^2} \sigma , \quad T_* \equiv \sqrt{m_\sigma M_H} , \quad u \equiv \frac{T}{T_*} , \quad \frac{\mathrm{d}^2 \omega}{\mathrm{d}u^2} + \frac{\omega}{u^6} + \frac{1}{u^2} = 0 . \quad (D1)$$

A general solution takes the form

$$\omega(u) = \omega_0(u) + c_1 \omega_1(u) + c_2 \omega_2(u) , \qquad (D2)$$

where coefficients c_1 and c_2 are determined by the boundary conditions, and where

$$\omega_0(u) = \frac{\pi}{\Gamma(1/4)\sqrt{u}} J_{-\frac{1}{4}} \left(\frac{1}{2u^2}\right) {}_{1}F_{2} \left(\frac{1}{4}; \frac{5}{4}, \frac{5}{4}; -\frac{1}{16u^4}\right)
+ \frac{\pi\sqrt{u}}{8} J_{\frac{1}{4}} \left(\frac{1}{2u^2}\right) G_{1,3}^{2,0} \left(\frac{1}{16u^4} \middle| 0, 0, \frac{1}{4} \right) ,$$
(D3)

$$\omega_1(u) = \Gamma(3/4)\sqrt{\frac{u}{2}}J_{-\frac{1}{4}}\left(\frac{1}{2u^2}\right), \qquad \omega_2(u) = \Gamma(5/4)\sqrt{2u}J_{\frac{1}{4}}\left(\frac{1}{2u^2}\right).$$
 (D4)

The function ω_0 is expressed in terms of hypergeometric F and Meijer G functions. A plot of the functions $\omega_{0,1,2}$ is shown in Figure 4.

At high temperatures $u \gg 1$, the functions ω_i have asymptotic series expansions:

$$\omega_0(u) \rightarrow \ln u + 1.2774 - \frac{\ln u}{20u^4} - \frac{0.0864}{u^4} + \mathcal{O}(u^{-8}) ,$$
 (D5)

$$\omega_1(u) \rightarrow u - \frac{1}{12u^3} + \mathcal{O}(u^{-7}) ,$$
 (D6)

$$\omega_2(u) \rightarrow 1 - \frac{1}{20u^4} + \mathcal{O}(u^{-8}) \ .$$
 (D7)

These solutions correspond to the era in which the flavon mass is small compared to the Hubble rate, $H \gg m_{\sigma}$, so that the $m_{\sigma}^2 \sigma$ term in (14) is negligible.

When the temperature drops below $u \lesssim 1$, the flavon mass becomes relevant and the field begins to oscillate. In this limit the solutions ω_i are well approximated by

$$\omega_0(u) \approx 1.607u^{3/2}\cos\left(\frac{1}{2u^2} - \frac{\pi}{8}\right) ,$$
 (D8a)

$$\omega_1(u) \approx 0.978u^{3/2}\cos\left(\frac{1}{2u^2} - \frac{\pi}{8}\right) ,$$
 (D8b)

$$\omega_2(u) \approx 1.446u^{3/2}\cos\left(\frac{1}{2u^2} - \frac{3\pi}{8}\right) ,$$
 (D8c)

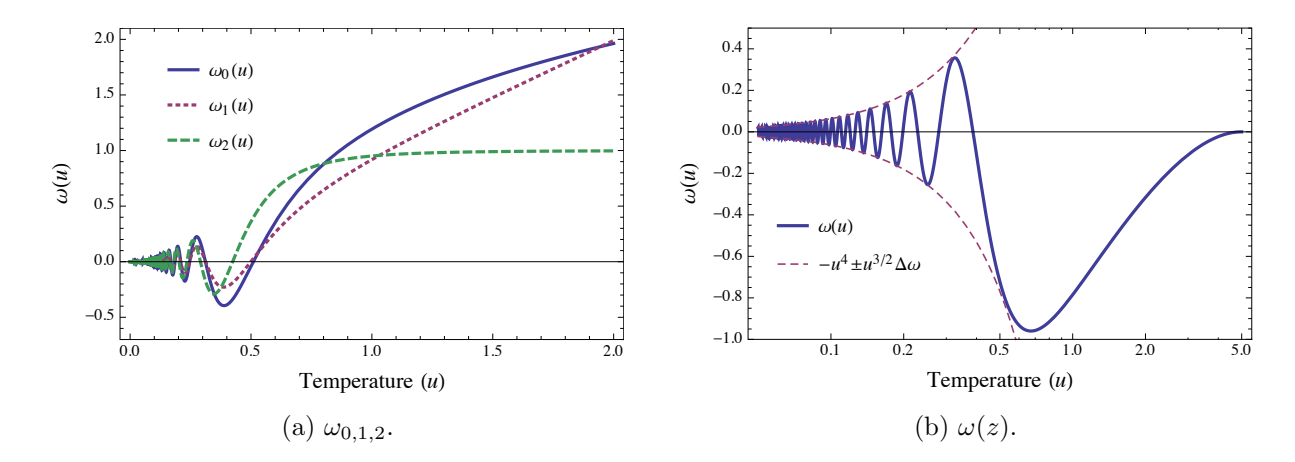


FIG. 4. In (a) we show the three functions $\omega_{0,1,2}$ which enter into the general solution, $\omega = \omega_0 + c_1\omega_1 + c_2\omega_2$. In (b) we take the initial condition $\omega(u_0) = \omega'(u_0) = 0$ at $u_0 = 5.0$. The dashed lines represent the envelope $-u^4 \pm u^{3/2}\Delta\omega$, which accurately describes the low-temperature (u < 1) oscillation about the minimum of the finite-temperature scalar potential.

which satisfy the low-temperature limit of (D1), $u^2 \frac{d^2 \omega}{du^2} + \omega/u^4 = \mathcal{O}(u^{3/2}) \ll 1$. Conveniently, the phases of ω_0 and ω_1 approach each other as $u \to 0$, so that the amplitude of the total oscillation can be written in terms of c_1 and c_2 :

$$\omega(u) = -u^4 + u^{3/2} \Delta \omega \cos\left(\frac{1}{2u^2} - \phi_0\right) , \qquad (D9a)$$

$$\Delta\omega^2 = (1.607 + 0.978c_1)^2 + (1.446c_2)^2 + 2.045(1.607 + 0.978c_1)c_2,$$
 (D9b)

where the phase ϕ_0 of the general solution is also determined by c_1 and c_2 . At temperatures $H \lesssim m_{\sigma}$, the flavon oscillates about the minimum of its finite-temperature scalar potential, $\omega = -u^4$, rather than $\omega = 0$: this distinction becomes important for small reheating temperatures $T_R \ll \sqrt{m_{\sigma} M_H}$.

Given specific boundary conditions $\omega(u_0)$ and $\omega'(u_0)$ at some initial $u_0 = T_R/\sqrt{m_\sigma M_H}$, the coefficients c_1 and c_2 can be derived from the exact solutions ω_i . For $u_0 \gg 1$ it is easier to use the asymptotic solution $\omega(u) \simeq \ln u + c_1 u + c_2 + 1.277$ instead, with the result

$$c_1 = \omega'(u_0) - \frac{1}{u_0}$$
 and $c_2 = \omega(u_0) - u_0 \,\omega'(u_0) - \ln u_0 - 0.277$. (D10)

As we discuss in Section III A, a modest lower bound on the amplitude of the oscillation can be found by assuming the initial condition $\omega(u_0) = \omega'(u_0) = 0$, which corresponds to the $u \gg 1$ asymptotic solution $\omega(u) = \ln(u/u_0) - u/u_0 + 1$. The amplitude of the oscillations when the temperature falls below $u \lesssim 1$ can be taken simply from (D9b). More general initial conditions such as $\omega'(u_0) \neq 0$ typically produce larger oscillations, though it is possible to fine-tune the initial conditions such that it is suppressed.

If the reheating temperature is small to begin with, $u_0 \ll 1$, the flavon oscillates freely about the minimum of its finite temperature potential, $\omega(u) = -u^4$. Taking the $\omega(u_0) = \omega'(u_0) = 0$ initial condition, the amplitude of the flavon oscillations is $u_0^{5/2}u^{3/2}$. The left panel of Figure 5 shows $\omega(u)$ with $u_0 = 0.2$, along with the envelope function $-u^4 \pm \Delta\omega$

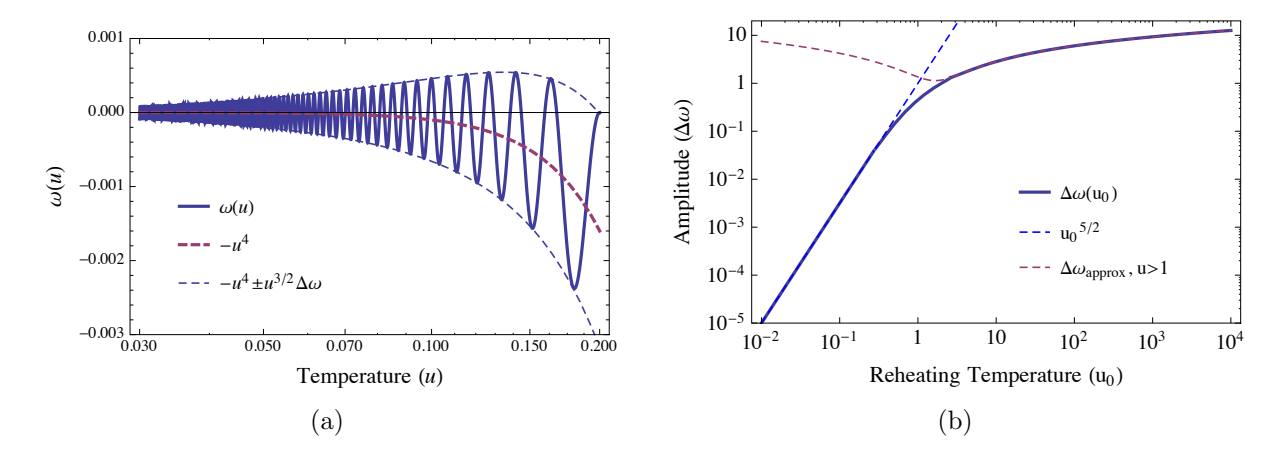


FIG. 5. In (a) we take $\omega(0.2) = \omega'(0.2) = 0$, and show that for low reheating temperatures ($u_0 \ll 1$) the flavon oscillates about $\omega = -u^4$ with an amplitude proportional to $u_0^{5/2}u^{3/2}$. In (b) we plot the amplitude $\Delta\omega$ of the flavon oscillations as a function of the rescaled reheating temperature, u_0 , again using the assumption that the flavon begins at rest at the minimum of its zero-temperature scalar potential. The solid blue line utilizes the exact solution to the equations of motion; the dotted lines show the low-temperature and high-temperature approximations, respectively.

with
$$\Delta\omega = u_0^{5/2}$$
.

In the intermediate range $0.4 \lesssim u_0 \lesssim 2.0$, we find the flavon amplitude $\Delta \omega$ by solving for c_1 and c_2 exactly. This result is shown in the right panel of Figure 5 along with the $u_0 \ll 1$ and $u_0 \gg 1$ approximations to $\Delta \omega$.

As in freeze-in flavon production, it is convenient to use the flavon yield $Y_{\sigma} = n_{\sigma}/s$ to describe the flavon abundance. From (D9b), it can be seen that Y_{σ} is constant with respect to temperature,

$$Y_{\sigma} = \frac{\rho_{\sigma}}{m_{\sigma}s} = \alpha^2 \frac{A_{\star} M_{\rm P} m_{\sigma}}{\Lambda^2} \left(\frac{M_H}{m_{\sigma}}\right)^{3/2} \Delta \omega^2 , \qquad (D11)$$

where

$$\Delta\omega^{2} = \begin{cases} (T_{R}/T_{*})^{5} & \text{for } T_{R} \lesssim \frac{1}{2} T_{*}, \\ 2.09 \ln^{2} (T_{R}/T_{*}) & \text{for } T_{R} \gtrsim 2 T_{*}. \end{cases}$$
(D12)

Appendix E: Freeze-In With Correct Statistical Factors

In thermal equilibrium, the phase space density for fermions or bosons is given by $f_{\psi,\phi}(E) = (e^{E/T} \pm 1)^{-1}$, with $E = \sqrt{p^2 + m^2}$ for massive particles. In the limit $T \ll m$, $f_{\psi,\phi}(E)$ both approach the Maxwell–Boltzmann (MB) distribution, $f_{\psi,\phi}(E) \approx e^{-E/T}$, which simplifies the Boltzmann equation significantly. For freeze-in processes driven by nonrenormalizable operators, however, the freeze-in yield is typically driven by high-temperature production, $T \sim T_R$, which in our case of weakly coupled flavons implies the relativistic limit, $T \gg m_{\sigma}$.

In this section, we use correct fermionic/bosonic statistics to calculate the contribution to the freeze-in yield from relativistic $q\bar{q} \to \sigma\Phi$ scattering, in order to estimate the error introduced by approximating them as Maxwell–Boltzmann. With its fermionic initial state and bosonic final state, this process receives the most significant modification from the statistical factors, and can therefore be used to infer an upper bound on the total freeze-in yield. Conveniently, the squared amplitude for this process is independent of the angular coordinates:

$$\left| \mathcal{M} \left(q_i \bar{q}_j \to \sigma \Phi^{(*)} \right) \right|^2 = \frac{24 \left| g_{ij}^{u/d} \right|^2 s}{\Lambda^2} , \tag{E1}$$

where $s = (p_A + p_B)^2 = (p_1 + p_2)^2$. Here p_A and p_B refer to the momenta of the incoming quark and antiquark, while p_1 and p_2 refer to the flavon and Higgs doublet, respectively. The evolution of the flavon number density n_{σ} is given by the Boltzmann equation,

$$\dot{n}_{\sigma} + 3H n_{\sigma} = \int d\Pi_A d\Pi_B d\Pi_1 d\Pi_2 f_A(E_A) f_B(E_B) \left[1 + f_2(E_2) \right] \times (2\pi)^4 \delta^{(4)} (p_A + p_B - p_1 - p_2) |\mathcal{M}|^2 ,$$
 (E2)

where $d\Pi_i = \frac{d^3p_i}{(2\pi)^3 2E_i}$ is the Lorentz-invariant phase space. Defining the variables $E_+ = E_A + E_B$ and $E_- = E_A - E_B$, the initial state $d^3p_A d^3p_B$ integral simplifies to

$$d\Pi_A d\Pi_B = \frac{dE_+ dE_- ds}{2^7 \pi^4} \,. \tag{E3}$$

We also define $d^3p_2=(2\pi)E_2^2dE_2d\cos\theta_2$, where θ_2 is the angle between \vec{p}_2 and the center-of-mass 3-momentum $\vec{p}_1+\vec{p}_2$, so that the remaining $\delta(E_+-E_1-E_2)$ can be used to perform the angular integration. In terms of the dimensionless variables $z=\sqrt{s}/T$, $y=E_+/T$, $w=E_-/T$, and $\tau=E_2/T$, the Boltzmann equation is written:

$$\frac{\dot{n}_{\sigma} + 3Hn_{\sigma}}{T^{4}} = \frac{1}{2^{9}\pi^{5}} \int_{0}^{\infty} dz \, z \, |\mathcal{M}|^{2} \int_{z}^{\infty} \frac{dy}{\sqrt{y^{2} - z^{2}}} \int_{-\sqrt{y^{2} - z^{2}}}^{\mathbf{e}^{y}} \frac{dw}{1 + 2e^{y/2} \cosh \frac{w}{2}} \int_{\tau_{\min}}^{\tau_{\max}} \frac{d\tau}{1 - e^{-\tau}} ,$$
(E4)

where

$$\tau_{\text{max,min}} = \frac{y \pm \sqrt{y^2 - z^2}}{2} \ . \tag{E5}$$

Both the u and τ integrals can be completed analytically, with the result

$$\frac{\dot{n}_{\sigma} + 3Hn_{\sigma}}{T^{4}} = \frac{1}{2^{6}\pi^{5}} \int_{0}^{\infty} dz \, z \, |\mathcal{M}|^{2} \int_{z}^{\infty} \frac{dy}{\sqrt{y^{2} - z^{2}}} \\
\frac{\arctan\left(\tanh\frac{y}{4}\tanh\frac{\sqrt{y^{2} - z^{2}}}{4}\right)}{e^{y} - 1} \ln\left(\frac{\exp\frac{y + \sqrt{y^{2} - z^{2}}}{2} - 1}{\exp\frac{y - \sqrt{y^{2} - z^{2}}}{2} - 1}\right) .$$
(E6)

Noting that $|\mathcal{M}|^2 \sim z^2 T^2/\Lambda^2$, the above integral can be integrated numerically:

$$\frac{\dot{n}_{\sigma} + 3Hn_{\sigma}}{T^4} = \left(7.8 \times 10^{-4}\right) \times \frac{24g_{ij}^2 T^2}{\Lambda^2} \ . \tag{E7}$$

When the MB approximation is taken in Equation (E4), the result is smaller,

$$\frac{\dot{n}_{\sigma} + 3Hn_{\sigma}}{T^{4}} \approx \frac{1}{2^{9}\pi^{5}} \int_{0}^{\infty} dz \, z \, |\mathcal{M}|^{2} \int_{z}^{\infty} \frac{dy}{\sqrt{y^{2} - z^{2}}} \int_{-\sqrt{y^{2} - z^{2}}}^{\infty} \int_{\tau_{\min}}^{\tau_{\max}} d\tau \tag{E8}$$

$$\approx \frac{1}{2^8 \pi^5} \int_{0}^{\infty} dz \, z \, |\mathcal{M}|^2 z K_1(z) = \left(2.04 \times 10^{-4}\right) \times \frac{24 g_{ij}^2 T^2}{\Lambda^2} \,. \tag{E9}$$

Our use of Maxwell–Boltzmann statistics in Section IIIB causes us to underestimate the $Q_L \bar{q} \to \sigma \Phi$ scattering rate by a factor of 3.8.

Of the six processes identified in Equation (17), only the two with purely bosonic final states receive this factor of \sim four enhancement. To calculate the contributions from the remaining processes one must additionally perform the angular integral, which becomes nontrivial when the initial and final states both include a fermion. Considering that the total flavon yield is dominated by Y^{osc} rather than Y^{fl} in most of the parameter space, we leave this more precise determination of the relativistic freeze-in yield to future studies.

- [1] H. Georgi and S. L. Glashow, Phys. Rev. **D7**, 2457 (1973).
- [2] C. D. Froggatt and H. B. Nielsen, Nucl. Phys. **B147**, 277 (1979).
- [3] D. B. Kaplan, Nucl. Phys. **B365**, 259 (1991).
- [4] N. Arkani-Hamed and M. Schmaltz, Phys. Rev. **D61**, 033005 (2000), hep-ph/9903417.
- [5] T. Gherghetta and A. Pomarol, Nucl. Phys. **B586**, 141 (2000), hep-ph/0003129.
- [6] D. E. Kaplan and T. M. P. Tait, JHEP 11, 051 (2001), hep-ph/0110126.
- [7] Y. Grossman and M. Neubert, Phys. Lett. **B474**, 361 (2000), hep-ph/9912408.
- [8] M. Blanke, A. J. Buras, B. Duling, S. Gori, and A. Weiler, JHEP 03, 001 (2009), 0809.1073.
- [9] S. Casagrande, F. Goertz, U. Haisch, M. Neubert, and T. Pfoh, JHEP 10, 094 (2008), 0807.4937.
- [10] M. Bauer, S. Casagrande, U. Haisch, and M. Neubert, JHEP 09, 017 (2010), 0912.1625.
- [11] G. D. Coughlan, W. Fischler, E. W. Kolb, S. Raby, and G. G. Ross, Phys. Lett. 131B, 59 (1983).
- [12] B. de Carlos, J. A. Casas, F. Quevedo, and E. Roulet, Phys. Lett. B318, 447 (1993), hep-ph/9308325.
- [13] L. E. Ibanez and G. G. Ross, Phys. Lett. **B332**, 100 (1994), hep-ph/9403338.
- [14] P. Binetruy and P. Ramond, Phys. Lett. **B350**, 49 (1995), hep-ph/9412385.
- [15] V. Jain and R. Shrock, Phys. Lett. **B352**, 83 (1995), hep-ph/9412367.
- [16] E. Dudas, S. Pokorski, and C. A. Savoy, Phys. Lett. **B356**, 45 (1995), hep-ph/9504292.
- [17] Y. Nir, Phys. Lett. **B354**, 107 (1995), hep-ph/9504312.
- [18] P. Binetruy, S. Lavignac, and P. Ramond, Nucl. Phys. **B477**, 353 (1996), hep-ph/9601243.

- [19] M. Leurer, Y. Nir, and N. Seiberg, Nucl. Phys. B398, 319 (1993), hep-ph/9212278.
- [20] M. Leurer, Y. Nir, and N. Seiberg, Nucl. Phys. B420, 468 (1994), hep-ph/9310320.
- [21] P. Ramond, R. G. Roberts, and G. G. Ross, Nucl. Phys. **B406**, 19 (1993), hep-ph/9303320.
- [22] M.-C. Chen, D. R. T. Jones, A. Rajaraman, and H.-B. Yu, Phys. Rev. D78, 015019 (2008), 0801.0248.
- [23] M. B. Green and J. H. Schwarz, Phys. Lett. **149B**, 117 (1984).
- [24] W. Fischler, H. P. Nilles, J. Polchinski, S. Raby, and L. Susskind, Phys. Rev. Lett. 47, 757 (1981).
- [25] M. Dine, N. Seiberg, and E. Witten, Nucl. Phys. **B289**, 589 (1987).
- [26] K. Tsumura and L. Velasco-Sevilla, Phys. Rev. **D81**, 036012 (2010), 0911.2149.
- [27] M. Bauer, T. Schell, and T. Plehn, Phys. Rev. **D94**, 056003 (2016), 1603.06950.
- [28] L. Calibbi, Z. Lalak, S. Pokorski, and R. Ziegler, JHEP 07, 004 (2012), 1204.1275.
- [29] I. Baldes, T. Konstandin, and G. Servant, JHEP 12, 073 (2016), 1608.03254.
- [30] M. Bolz, A. Brandenburg, and W. Buchmüller, Nucl. Phys. B606, 518 (2001), hep-ph/0012052, [Erratum: Nucl. Phys.B790,336(2008)].
- [31] J. Pradler and F. D. Steffen, Phys. Rev. **D75**, 023509 (2007), hep-ph/0608344.
- [32] V. S. Rychkov and A. Strumia, Phys. Rev. **D75**, 075011 (2007), hep-ph/0701104.
- [33] L. Covi, H.-B. Kim, J. E. Kim, and L. Roszkowski, JHEP **05**, 033 (2001), hep-ph/0101009.
- [34] L. J. Hall, K. Jedamzik, J. March-Russell, and S. M. West, JHEP 03, 080 (2010), 0911.1120.
- [35] W. Buchmüller, K. Hamaguchi, and M. Ratz, Phys. Lett. **B574**, 156 (2003), hep-ph/0307181.
- [36] W. Buchmüller, K. Hamaguchi, O. Lebedev, and M. Ratz, Nucl. Phys. B699, 292 (2004), hep-th/0404168.
- [37] Y. Ema, D. Hagihara, K. Hamaguchi, T. Moroi, and K. Nakayama, (2018), 1802.07739.
- [38] M. Laine and A. Vuorinen, Lect. Notes Phys. **925**, pp.1 (2016), 1701.01554.
- [39] W. Hu and J. Silk, Phys. Rev. Lett. **70**, 2661 (1993).
- [40] J. Chluba, Mon. Not. Roy. Astron. Soc. 436, 2232 (2013), 1304.6121.
- [41] F. Iocco, G. Mangano, G. Miele, O. Pisanti, and P. D. Serpico, Phys. Rept. 472, 1 (2009), 0809.0631.
- [42] R. H. Cyburt, B. D. Fields, K. A. Olive, and T.-H. Yeh, Rev. Mod. Phys. 88, 015004 (2016), 1505.01076.
- [43] M. Kawasaki and T. Moroi, Prog. Theor. Phys. 93, 879 (1995), hep-ph/9403364.
- [44] R. H. Cyburt, J. R. Ellis, B. D. Fields, and K. A. Olive, Phys. Rev. D67, 103521 (2003), astro-ph/0211258.
- [45] M. Kawasaki, K. Kohri, and T. Moroi, Phys. Lett. **B625**, 7 (2005), astro-ph/0402490.
- [46] M. Kawasaki, K. Kohri, and T. Moroi, Phys. Rev. D71, 083502 (2005), astro-ph/0408426.
- [47] K. Jedamzik, Phys. Rev. **D74**, 103509 (2006), hep-ph/0604251.
- [48] M. Kawasaki, K. Kohri, T. Moroi, and Y. Takaesu, Phys. Rev. D97, 023502 (2018), 1709.01211.
- [49] R. Cooke, M. Pettini, R. A. Jorgenson, M. T. Murphy, and C. C. Steidel, Astrophys. J. 781, 31 (2014), 1308.3240.
- [50] Y. I. Izotov, T. X. Thuan, and N. G. Guseva, Mon. Not. Roy. Astron. Soc. 445, 778 (2014), 1408.6953.
- [51] E. Aver, K. A. Olive, and E. D. Skillman, JCAP **1507**, 011 (2015), 1503.08146.
- [52] M. Fukugita and T. Yanagida, Phys. Lett. **B174**, 45 (1986).
- [53] Y. Ema, K. Hamaguchi, T. Moroi, and K. Nakayama, JHEP **01**, 096 (2017), 1612.05492.
- [54] Planck Collaboration, P. A. R. Ade et al., Astron. Astrophys. 594, A13 (2016), 1502.01589.

- [55] L. Kofman *et al.*, JHEP **05**, 030 (2004), hep-th/0403001.
- [56] M. Berkooz, Y. Nir, and T. Volansky, Phys. Rev. Lett. 93, 051301 (2004), hep-ph/0401012.
- [57] Particle Data Group, C. Patrignani et al., Chin. Phys. C40, 100001 (2016).
- [58] F. Feroz, M. P. Hobson, and M. Bridges, Mon. Not. Roy. Astron. Soc. 398, 1601 (2009), 0809.3437.
- [59] W. Porod, Comput. Phys. Commun. **153**, 275 (2003), hep-ph/0301101.
- [60] W. Porod and F. Staub, Comput. Phys. Commun. 183, 2458 (2012), 1104.1573.
- [61] F. Staub, Comput. Phys. Commun. 185, 1773 (2014), 1309.7223.